CHAPTER VI

SOL-GEL DERIVED POROUS CERIA POWDERS USING CERIUM GLYCOLATE COMPLEX AND THEIR CHARACTERIZATION

Abstract

The preparation of ceria (cerium dioxide, CeO_2) powders via a sol-gel process using cerium glycolate complex as precursor has been considered. We have also studied the hydrolysis of cerium glycolate complex. The hydrolysis was followed by FTIR spectroscopy, and the evolution of the Ce-O-C bands of the cerium glycolate molecule was analyzed. The intensity of these bands decreased with the hydrolysis time. X-ray diffraction (XRD), N_2 adsorption (BET specific surface area), and scanning electron microscopy (SEM) techniques have been applied to characterize the texture and structure of ceria systems prepared by the sol-gel method containing different hydrolysis ratio and calcined at temperatures between 400 and 1100°C. Crystallization is observed only after thermal treatment at above 400°C. The thermal stability of ceria system is confirmed by obtaining moderate surface areas even after the high temperature of calcination.

Introduction

Cerium dioxide based materials have become one of the most important ceramic materials. It has a number of multiple applications, such as an electrolyte material of solid oxide fuel cells (SOFCs), a material of high refractive index, an ionic conductor, a gas sensor, and an insulating layer on silicon substrates.[1-7] Other promising applications of ceria-based materials include automotive catalysts, solid electrolyte oxygen pumps, SOFCs anode materials, and mixed conducting membranes for oxygen separation and partial oxidation of hydrocarbons.[8-14] Ceria powders have been reported to be synthesized by different techniques including hydrothermal synthesis,[15] precipitation method,[16-17] spray pyrolysis technique,[18] thermal decomposition of carbonates,[19] electrochemical method,[20] and microemulsion.[21] In the development of soft chemistry, the sol-gel process is one of the most promising ways to append functionalities to ceramic materials, because of a large number of advantages that it offers, including a low temperature technique, a simple process, and the maintenance of excellent control on the molecular level. This process usually consists of two governing reactions involving the hydrolysis and condensation of molecular precursors such as metal alkoxides to form the oxide network. [22-26]

Several researchers reported the approaches for metal oxides which are prepared from inorganic salts as precursor.[25, 27-29] However, the counter anions of the starting cerium salts may remain in the product and deteriorate the purity of the products . To avoid counter anion contamination, cerium alkoxides can be used as the starting material for the ceria materials. This is justified as alkoxide hydrolysis produced H_2O and eventually CO/CO_2 that are readily removed from the product by the subsequent calcinations following sol-gel synthesis. Only a few approaches to the formation of transition metal oxide gels through the hydrolysis of transition metal alkoxides, the major problem is to control hydrolysis and condensation rates which are generally too fast, resulting in the precipitates with a high degree of microstructural disorder.[30] Mazdiyasni et al.[31] hydrolyzed isopropoxides of lanthanides to form hydroxides. The major problem of this technique is that the synthesis of the alkoxide precursor is complicated and requires air- and water- free working environments. Additionally, these usual precursors are expensive.

Due to the shortcomings of metal alkoxides such as relatively high toxicity, cost and sensitivity to moisture, we used cerium glycolate complex as a starting precursor for preparing the ceria materials. Cerium glycolate is glycolate derivatives of cerium synthesized directly from the reaction of inexpensive and readily available compounds, cerium hydroxide and ethylene glycol, via the one step process. Its presence of glycolate ligands is hydrolytically stable, thus yielding more controllable chemistry and minimizing special handling requirement. Thus, it can be used as a candidate precursor for ceramic processing by sol-gel technique. In this contribution, the purpose of present work is to investigate the preparation of high surface area porous ceria powders using sol-gel route and to study the hydrolysis of cerium glycolate synthesized via the oxide one pot synthesis process. To accomplish that goal, the influence of hydrolysis ratio on the crosslinking process and subsequent thermal treatment were also elucidated.

Experimental section

Materials. Cerium (IV) hydroxide ($Ce(OH)_4$) containing 87.4% CeO_2 as determined by TGA was obtained from Sigma-Aldrich Chemical Co. Inc. (USA) and sodium hydroxide was purchased from Merck Company Co. Ltd. (Germany). Both were used as received. Ethylene glycol (EG), used as reactant and solvent in the reaction, was purchased from Farmitalia Carlo Erba (Barcelona) and purified by fractional distillation at 200°C, under nitrogen at atmospheric pressure prior to use. Triethylenetetramine (TETA) was obtained from Facai Polytech. Co. Ltd. (Bangkok, Thailand) and distilled under vacuum (0.1 mmHg) at 130°C before use. Acetonitrile was purchased from Lab-Scan Company Co. Ltd. and purified by distilling over calcium hydride powder. Nitric acid used as catalyst in sol-gel process was purchased from Lab-Scan Company Co. Ltd.

Instruments. Fourier transform infrared (FT-IR) spectra were recorded on a VECTOR3.0 BRUKER spectrophotometer with a spectral resolution of 4 cm^{-1} to examine functional groups of the synthesized precursor. The solid sample was obtained using transparent KBr pellet containing 1% of sample mixed with 99%

dried KBr. Thermal behavior and stability of the synthesized precursor were investigated by thermogravimetric analysis (TGA) and differential scanning calorimetry (DSC) analysis. TGA was conducted on a TGA7 Perkin-Elmer thermal analysis system with a heating rate of 10°C min^{-1} over 30 – 1200°C temperature range. DSC analysis was obtained on a Netzsch DSC200 (Germany) from 25 to 500° C at the heating rate of 10° C min^{-1}. ^{1}H- and ^{13}C-NMR spectra of the synthesized precursor were performed with a Bruker 200 MHz spectrometer at the Chemistry Department, Faculty of Science, Chulalongkorn University, using deuterated dimethyl sulfoxide (DMSO-d_6) as solvent and reference for chemical shift measurements at room temperature. Variable temperature NMR spectra of the synthesized precursor were characterized on a JEOL 500 MHz spectrometer in the temperature range 25 – 140°C. To examine the molar mass of synthesized precursor, mass spectrum was carried out on a Fison Instrument (VG Autospec-ultima 707E) with VG data system, using the positive fast atomic bombardment mode (FAB^{+}-MS) with glycerol as the matrix, cesium gun as initiator, and cesium iodide (CsI) as a standard for peak calibration. Elemental analysis (EA) was performed on a C/H/N analyzer (Perkin Elmer PE2400 series II) to obtain the product composition. The gelation of cerium glycolate precursor was examined by an FT-IR spectrophotometer (Nicolet, NEXUS 670). The change of obtained gels during the thermal treatment was investigated by Simultaneous thermal analysis (STA) using a Netzsch STA 409 Instrument. The textural properties and porosity of ceria materials were explored by adsorption of nitrogen at 77 K with Autosorb-1 gas sorption instrument (Quantasorb JR.). A Rigku D/Max-2200 Powder Diffractometer was used to determine X-ray diffraction patterns of the calcined products.

Precursor preparation. Cerium glycolate precursor was prepared according to a previous work.[32] The synthesis of cerium glycolate was carried out in one step by mixing cerium hydroxide (5.3 mmol of CeO_2), and triethylenetetramine (5 mmol) with sodium hydroxide at about 12 mol % equivalent to cerium hydroxide in a simple distillation set using 18 cm^3 of ethylene glycol. The reaction mixture was heated to the boiling point of ethylene glycol for 18 h under nitrogen atmosphere to remove the by-product water and ethylene glycol from the reaction. The reaction

mixture was cooled at room temperature. The precipitated product was separated, washed with acetonitrile and dried under vacuum (0.1 mmHg) at room temperature. The resulting product was characterized using FT-IR, TGA, DSC, EA, NMR and MS.

Sol-gel process of synthesized cerium glycolate precursor. The studied materials were prepared via the sol-gel procedure by hydrolyzing cerium glycolate precursor with the mixture of nitric acid and water at various acid contents. Three hydrolysis ratio (h=[H_2O]/[Ce]) of 4, 8, 12 were studied while the acid ratio (A = [acid]/[Ce]) was kept constant at the value of 0.25 due to gellability zone. The gelation reaction was carried out at room temperature and maintaining a stirring during the whole process.

Ceria powders were produced by heat treatment of the resulting gels at various hydrolysis ratio in a furnace in the temperature range 400 - 1100°C and held at the final temperature for 7 hours.

FT-IR spectroscopic investigation of cerium glycolate gelation. The hydrolysis and condensation of cerium glycolate during sol-gel process as a function of the reaction time were followed by means of Fourier-transform IR spectroscopy.[33] An FT-IR spectrophotometer (Nicolet, NEXUS 670) with 16 scans at a resolution of 4 cm^{-1} using Zn-Se window cell was used in this study. Data acquisition and processing were performed using an Omnic software package.

Characterization of calcined products. Thermal decomposition and change of the ceria-based gels during the thermal treatment were investigated by thermogravimetry (TG/DSC) using a Netzch STA409 equipment. Samples were heated in an alumina crucible at the temperature range for scanning from 30 to 1200°C and the scanning speed was 10°C min^{-1}. The porous structure of ceria obtained after calcination was characterized by nitrogen adsorption technique. The adsorption/desorption isotherms of nitrogen at 77 K were recorded with an Autosorb-1 Gas Sorption Instrument (Quantachrome Corporation). All sample were previously subjected to an outgas treatment at 250°C under a reduced pressure before adsorption

measurements. Specific surface area was calculated according to BET theory, and the total pore volume was determined from the amount of nitrogen adsorbed at pressure close to saturation. Pore size distribution was obtained taking into account the desorption branch of the isotherm. Sample microstructure was investigated by Scanning Electron Microscopy (SEM) carried out on a JEOL 5200-2AE apparatus. Samples of the materials were mechanically deposited on the holders and subsequently gold coated to reduce charge buildup. The sample was then transported to the microscope stage and the equipment was pumped down for a period before observation. The structure of the phases in the samples calcined at various temperatures was identified by X-ray diffraction using a D/MAX 2000 series (Rigaku Co.) powder diffractometer. The samples were scanned at room temperature over angular range $5^{o} < 2\theta < 90^{o}$ at 5^{o} min^{-1} scan rate using Cu Kα radiation (λ = 0.154 nm) by placing samples in glass sample holder. The Scherrer method was employed to estimate the grain or crystallite size of the crystalline calcined products.

Results and Discussion

Precursor preparation. Cerium glycolate complex was successfully synthesized by the oxide one pot synthesis process directly from cerium hydroxide and ethylene glycol. The reaction is the condensation reaction, liberating water as a by-product. The high percentage yield of the product was thus obtained by slowly distilling off the excess ethylene glycol at atmospheric pressure to remove water from the system.

The FT-IR spectrum of the obtained cerium glycolate complex shows the following absoption bands: 2939-2873 cm^{-1} (γ(C-H)) and 1080 cm^{-1} (γ(C-O-Ce)). The ^{1}H- NMR spectrum shows one singlet peak at 3.4 ppm referring to chelated glycolate ligands of CH_2-O-Ce. Similarly, one singlet peak appears in the ^{13}C-NMR at 62.8 ppm belonging to the symmetrical carbons of chelated glycolate ligand (CH_2-O-Ce). Elemental analysis found that the resulting percentages of carbon and hydrogen are consistent with the theoretical values, found (%): C, 18.28; and H, 3.08 and anal. calcd. (%): C, 18.45; and H, 3.08. FAB^{+}-MS spectrum shows the base peak at m/e 184 belonging to the structure of $[CeC_2H_4O]^{+}$ and approximately 15% intensity of the molecular peak at m/e 262 corresponding to $[CeC_4H_8O_4]$-$2H^{+}$. DSC

result exhibits one exotherm peak at 410°C corresponding to decomposition of all organic ligands. Similarly, TGA analysis appears one thermal decomposition transition at around 350-525°C with 65.9% ceramic yield in agreement with $Ce(OCH_2CH_2O)_2$ structure having the calculated ceramic yield 66.1%.

Hydrolysis of cerium glycolate precursor by FTIR technique. The hydrolysis of cerium glycolate molecule can be followed by the FTIR bands situated at 1080 and 690 cm^{-1} corresponding to the Ce-O-C and Ce-O-Ce groups, respectively as it is shown in Fig. 1. The intensity of γ (Ce-O-C) stretching vibration of cerium glycolate complex at 1080 cm^{-1} decreased continuously with the reaction time. The starting cerium glycolate precursor can also be observed at 0 min in the spectral range 800 – 500 cm^{-1}. These bands indicating to C-H, C-O and Ce-O-C deformation vibrations diminished, whilst the intensity and width of this spectral range increased as the reaction time increased. This result corresponded to the formation of Ce-O-Ce bonds due to the condensation reaction. The FTIR spectra of hydrolyzed cerium glycolate precursor at different hydrolysis ratio were exhibited in Fig.1. The intensity of Ce-O-Ce was maximized at h = 12 with decreasing the intensity at lower hydrolysis ratio. The decrease in intensity of Ce-O-C band is accompanied with the increase of Ce-O-Ce band as hydrolysis ratio increases. This implies that the effect of an increase of the hydrolysis ratio is an enhancement of the hydrolysis kinetic rate leading to the reduction of the gel time.

The above results give only qualitative information for the hydrolysis of cerium glycolate precursor. We have carried out a semiquantitative approach by a careful deconvolution of the FTIR profiles using a computer program. The results of the analysis are exhibited in the relationship between the peak ratio of Ce-O-C band (1080 cm^{-1}) and Ce-O-Ce band (690 cm^{-1}) with time (Fig. 2). This is only a semiquantitative profile of the gelation of cerium glycolate molecule. Generally, the reaction time is decreased by factors that increase the condensation rate. It is obvious that value of hydrolysis ratio is an important factor affecting the gel time. The results obtained here compared favorably with earlier study by qualitative FTIR.

Characterization of calcined gels. To provide an indication of suitable heat treatment temperature for ceria gels, bulk gel samples were characterized by thermogravimetry (TG-DSC) using a Netzsch STA equipment. The TG-DSC patterns in Fig.3 show the thermal behavior of the ceria gel heated up to 1200°C. The weight loss in the low temperature range (below 200°C) is due to the removal of water and gives rise to an endothermic peak in the corresponding DSC curve. The weight loss in the temperature range 200-380°C is attributed to the combustion or decomposition of residual organics formed by hydrolysis and condensation during the preparation of gels. This is supported by the presence of one exothermic peak at above 200°C to around 380°C in the DSC curve. Moreover, this exothermic peak emerged was also caused by the oxidation of Ce compound and formation of CeO_2. This is confirmed by the XRD results given in Fig. 4, where the organic residues were completely removed from the ceria gel and CeO_2 phase is formed above 400°C.

The XRD patterns of calcined samples are shown in Figure 4. For the sample annealed at 400°C, the diffraction peaks of organic residues disappear, and the amorphous feature emerged. Upon further increasing the annealing temperature to 500°C, XRD patterns of the heated sample show them to be single phase, all the reflections corresponding to those of cubic ceria (JCPDS file No. 34-394) having a fluorite type structure with space group *Fm3m* and fcc lattice constant a = 0.541 nm. After applying the Scherrer formula to the (111) diffraction peak of cerium oxide,[34] the crystallite sizes of cerium oxides as a function of calcination temperature are reported in Figure 5. The sintering of CeO_2 crystallites is particularly evident in the temperature above 700°C with a narrowing of the diffraction peaks, indicating an increase of particle dimensions. This is also in agreement with the loss of surface area observed following calcinations at temperatures higher than 700°C. The peak sharpness and intensity increased with temperature indicating an improvement in crystallinity of ceria. Fig. 6 shows the X-ray diffraction pattern of the calcined ceria powders at 600°C with the different hydrolysis ratio. In addition, it is worth to note that the crystallinity decreased with increasing hydrolysis ratio. According to the gelation process, when the hydrolysis ratio was increased, the gelation time decreased. The increase in water available for hydrolysis increased the number of Ce-OH groups present. The increase in this group accelerated the condensation

reaction, thus decreasing the gelation time. The higher hydrolysis ratio provided less time to arrange itself leading to lower crystallization.

BET surface areas obtained after thermal treatment under air at increasing temperatures are reported in Fig. 7. XRD measurements indicate that the loss in surface area at high temperatures is due to an increase in the size of crystallite domains from a value of 6-13 nm, observed after calcinations at 500°C to 32-35 nm, observed after calcinations at 900 °C (Fig. 5). This is also in agreement with the loss of surface area observed following calcinations at temperatures higher than 700°C. It is also noted that the smaller the hydrolysis ratio, the lower the surface area. Longer gelation times increased the crystallinity while decreasing the surface area. The general shape of the curves is the same. The BET specific surface area increases with the hydrolysis ratio from 132 to 170 m^2 g^{-1} (Fig.7). It can be implied that sol-gel process provides a larger specific surface area which decreases with increasing calcinations temperature and decreasing hydrolysis ratio. Figure 8 is an example of these measurements for the system with the hydrolysis ratio h = 12 and calcination temperature of 900°C. The adsorption-desorption isotherm of this sample showed no significant hysteresis, and the pore distribution was broad and composed of mesopores.

Fig. 9 show SEM observation results for CeO_2 prepared with different hydrolysis ratio. The calcined products obtained from ceria gels at lower hydrolysis ratio formed more perfect crystallines, as shown in Fig. 9, compared very well with the XRD results. When the calcinations temperature is raised, SEM micrographs (Fig. 10) indicated that the crystals begin to sinter and agglomerate together affecting the crystallite sizes and surface areas. From these results, it can be concluded that the lower hydrolysis ratio causes the better morphology that the higher hydrolysis ratio due to lower hydrolysis and condensation rates.

Conclusions

The sol-gel synthesis method provides the ceria system with thermal stability, using inexpensive and moisture-stable cerium glycolate complex as precursor. The FTIR technique was found to be effective for studying the gelation of cerium glycolate precursor. The hydrolysis ratio affected the gel time. An increase of

hydrolysis ratio leads to the reduction of gel time. Higher hydrolysis ratio also resulted in larger BET specific surface area. We show here that for materials with a very strong tendency to crystallize. It was concluded that the cubic fluorite structure was only existed in samples from results by XRD without other phases. In all of the samples, the crystallite size of synthesized CeO_2 increased with increasing calcination temperature. Heat treatment of the resulting ceria gels at 400°C produces a homogeneous ceria having high surface area.

Acknowledgments

This work was supported by the Thailand Research Fund (TRF), Postgraduate Education and Research Program in Petroleum and Petrochemical Technology, PPT consortium (ADB) Fund and Ratchadapisake Sompote Fund, Chulalongkorn University.

References

1. H. J. Beie and A. Gnorich, Sens. Actuators B., 4 (1991) 393-399.
2. A. Atkinson, Solid State Ionics, 95 (1997) 249.
3. B. C. H. Steele, Solid State Ionics, 129 (2000) 95.
4. A. E. C. Palmqvistl, M. Wirde, U. Gelius and M. Muhammed, Nanostruct. Mater., 11 (1999) 995.
5. J. Qiao and C. Y. Yang, Mater. Sci. Eng. R14 (1995) 157.
6. M. Ogita, K. Higo, Y, Nakanishi and Y. Hatanaka, Appl. Surf. Sci. 175 (2001) 721.
7. J. Sheng, N. Yoshida, J. Karasawa and T. Fukami, Sens. Actuators B 41 (1997) 131.
8. D. S. Bae, B. Lim, B. I. Kim and K. S. Han, Mater. Lett. 56 (2002) 610-613.
9. T. Tsuzuki, P. McCormick, J. Am. Ceram. Soc. 84 (7) (2001) 1453-1458.
10. Y. I. Matatov-Meytal and M. Sheintuch, Ind. Eng. Chem. Res. 37 (1998) 309.
11. W. Liu and M. Flytzani-Stephanopoulos, J. Catal. 153 (1995) 317.
12. M. Sahibzaba, B. C. H. Steele, K. Zheng, R. A. Rudkin, I. S. Metcalfe, Catal. Today 38 (1997) 459.

13. V.V. Kharton, A.A. Yaremchenko, E.N. Naumovich and F.M.B. Marques, J. Solid State Electrochem. 4 (2000) 243.
14. V.V. Kharton, A.V. Kovalesvsky, A.P. Viskup, F.M. Figueiredo, A.A. Yaremchenko, E.N. Naumovich and F.M.B. Marques, J. Electrochem. Soc 147 (2000) 2814.
15. M. Hirano, E. Kato, J. Am. Ceram. Soc. 79 (1996) 777.
16. E. Abi-add, R. Bechara, J. Grimblot, A. Aboukais, Chem. Mater. 5 (1993) 793.
17. L.A. Bruce, M. Hoang, A.E. Hughes, T.W. Turney, Appl. Catal. A: General 134 (1996) 351.
18. R.M. Vallet, F. Conde, S. Nicolopoulous, C.V. Ragel, J.M. Gonzales-Calbet, Mater. Sci. Forum. 235-238 (1997) 291.
19. M. Pijalot, J.P. Viricelle, M. Soustelle, Stud. Surf. Sci Catal. 91 (1995) 885.
20. Y. Zhou, R.J. Phillips, J.A. Switzer, J. Am. Ceram. Soc. 78 (1995) 981.
21. T. Matsui, K. Fujiwara, K. Machida, G. Adachi, T. Sakata, H. Mori, Chem. Mater. 9 (1997) 2197.
22. C.J. Brinker, G.W. Scherer, Sol-Gel Science: The Physics and Chemistry of Sol-Gel Processing, Academic Press, San Diego, 1990.
23. O. Harizanov, T. Ivanova, A. Harizanova, Mater. Lett. 49 (2001) 165.
24. A. Hernandez, L.M. Torres-Martinez, T. Lopez, Mater. Lett. 45 (2000) 340.
25. J.S. Lee, T. Matsubara, T. Sei, T. Tsuchiya, J. Mater. Sci. 32 (1997) 5249.
26. K. Izumi, M. Murakami, T. Deguchi, A. Morita, J. Am. Ceram. Soc. 72 (1989) 1465.
27. R.D. Purohit, B.P. Sharma, K.T. Pillai, A.K. Tyagi, Mater. Res. Bull. 36 (2001) 2711.
28. D. Terribile, A. trovarelli, J. Llorca, C.D. Leitenburg, G. Dolcetti, J. Catal. 178 (1998) 299.
29. K. Konstantinov, I. Stambolova, P. Peshev, B. Darriet, S. Vassilev, Inter. J. Inor. Mater. 2 (2000) 277.
30. J. Blanchard, S. Barboux-Doeuff, J. Maquet, C. Sanchez, New J. Chem. 19 (1995) 929.
31. K.S. Masdiyasni, L.M. Brown, J. Am. Ceram, Soc., 54 (1971) 479.
32. B. Ksapabutr, E. Gulari, S. Wongkasemjit, Mater. Chem. Phys., 83 (2004) 34.

33. B. Ksapabutr, E. Gulari, S. Wongkasemjit, Colloids&Surfaces A: Physicochem. Eng. Aspects, 233 (2004) 145.

34. J.S. Lee, S.C. Choi, Mater. Lett., 58 (2004) 390.

Figure Captions

Figure 1. FTIR spectra of ceria gel during sol-gel process at various hydrolysis ratio of (a) h = 12; (b) h = 8; (c) h = 4.

Figure 2. Variation of hydrolyzed cerium glycolate complex as a function of the reaction time at different hydrolysis ratio.

Figure 3. TG-DSC curves of the ceria gel obtained from the hydrolysis ratio of 12

Figure 4. X-ray diffraction patterns of hydrolyzed cerium glycolate precursor at various calcination temperatures of (a) 400°C, (b) 500°C, (c) 600°C, (d) 700°C, (e) 800°C, (f) 900°C and (g) 1100°C.

Figure 5. The crystallite sizes of the CeO_2 powders obtained at different hydrolysis ratio (h = 12, 8, and 4) and various calcination temperatures (500, 600, 700, 800, 900 °C)

Figure 6. X-ray diffraction patterns of CeO_2 powders at various hydrolysis ratio: (a) h = 12; (b) h = 8; (c) h = 4.

Figure 7. Effect of treatment temperature on the BET specific surface area of CeO_2 powders prepared with different hydrolysis ratio

Figure 8. Plots showing (a) Pore size distribution; (b) Nitrogen adsorption/ desorption isotherms of the alumatrane gel pyrolyzed at 500°C for 7 h.

Figure 9. Scanning electron micrographs of CeO_2 powders prepared at various hydrolysis ratio: (a) h = 12; (b) h = 8; (c) h = 4.

Figure 10. Scanning electron micrographs of CeO_2 powders after calcining at (a) 500°C, (b) 700°C, (c) 900°C and (d) 1100°C.

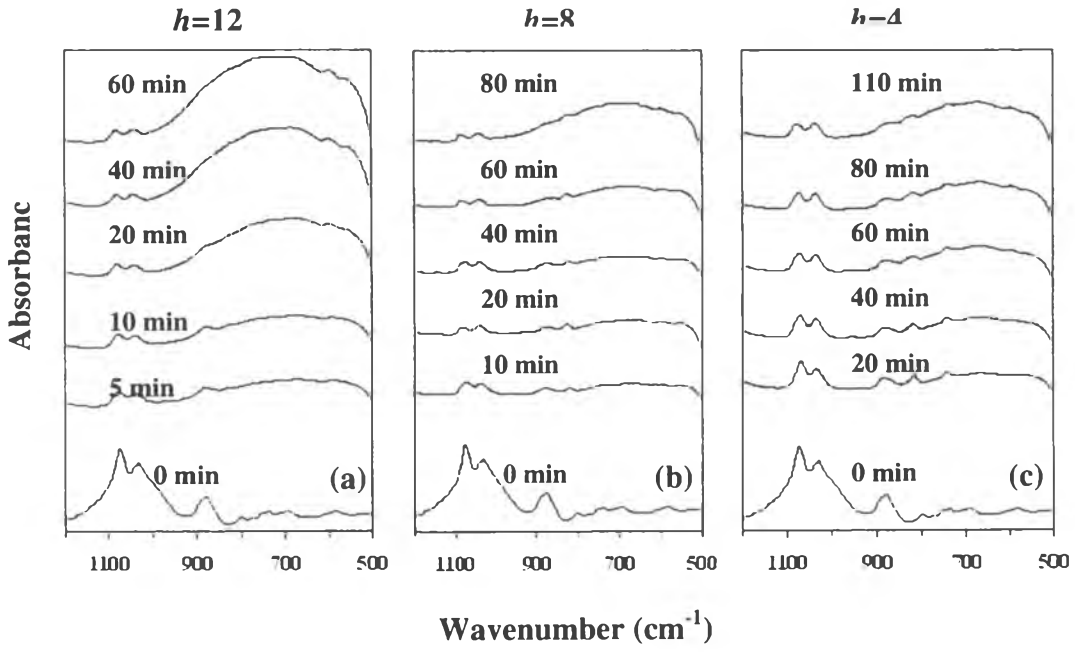

Figure 1. (Ksapabutr et al.)

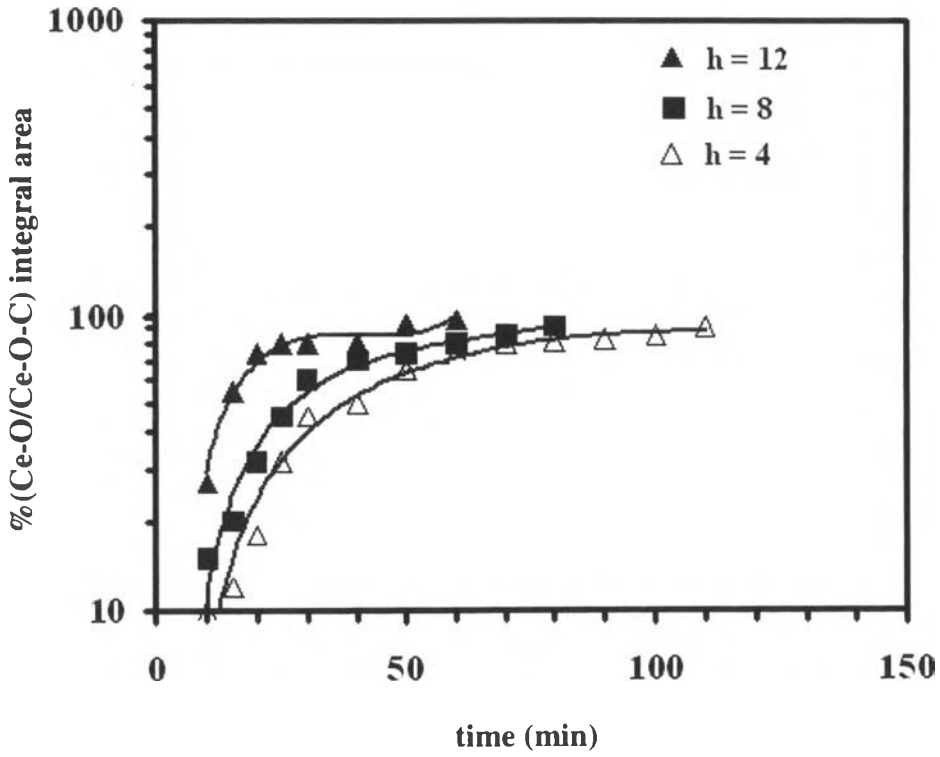

Figure 2. (Ksapabutr et al.)

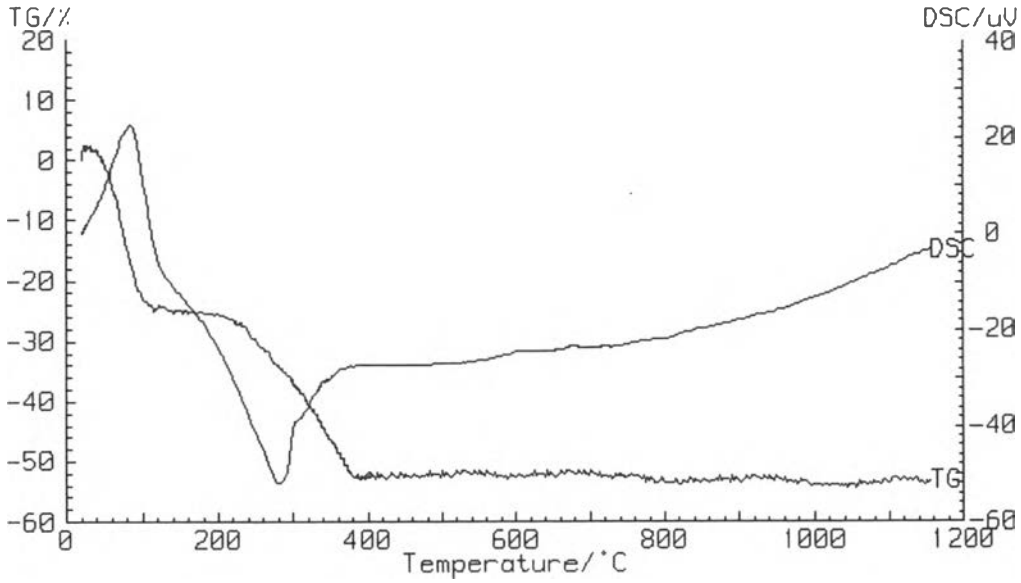

Figure 3. (Ksapabutr et al.)

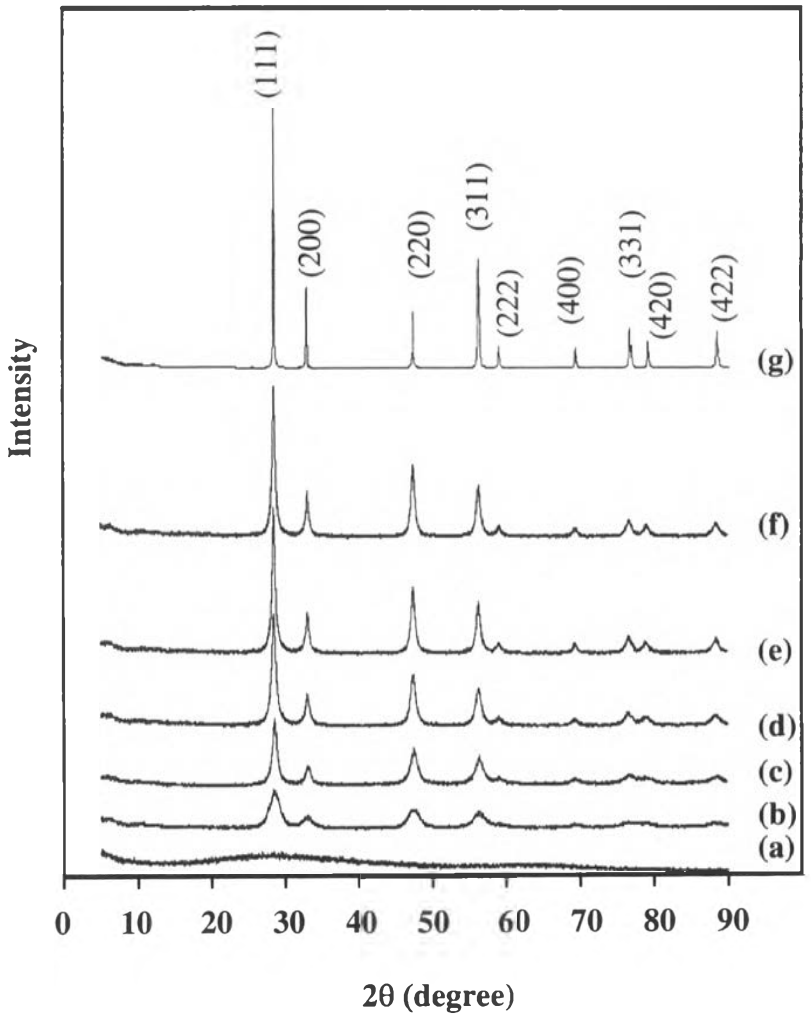

Figure 4. (Ksapabutr et al.)

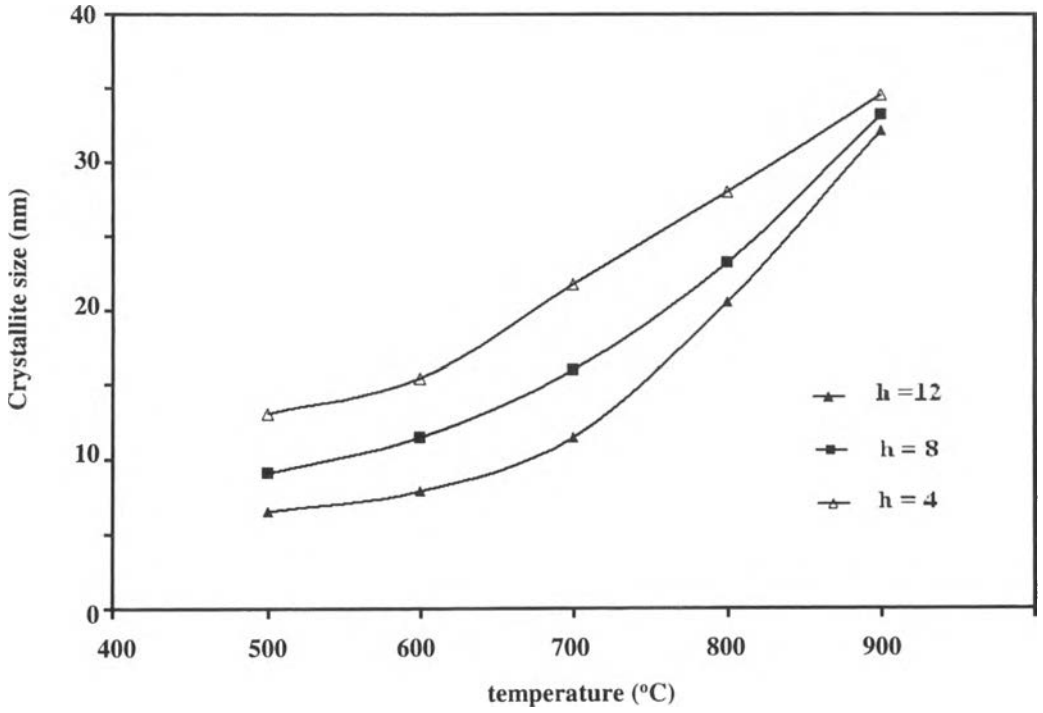

Figure 5. (Ksapabutr et al.)

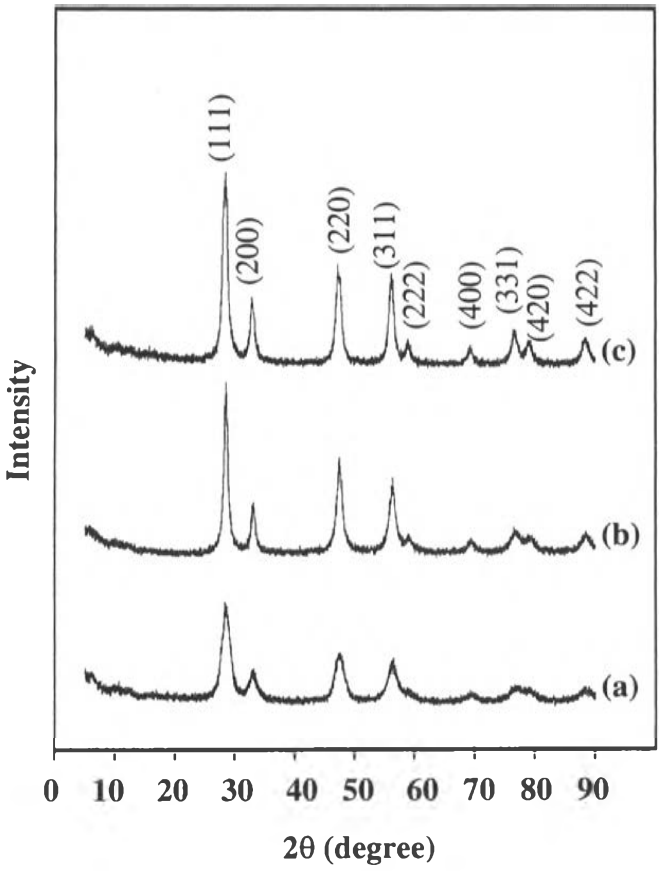

Figure 6. (Ksapabutr et al.)

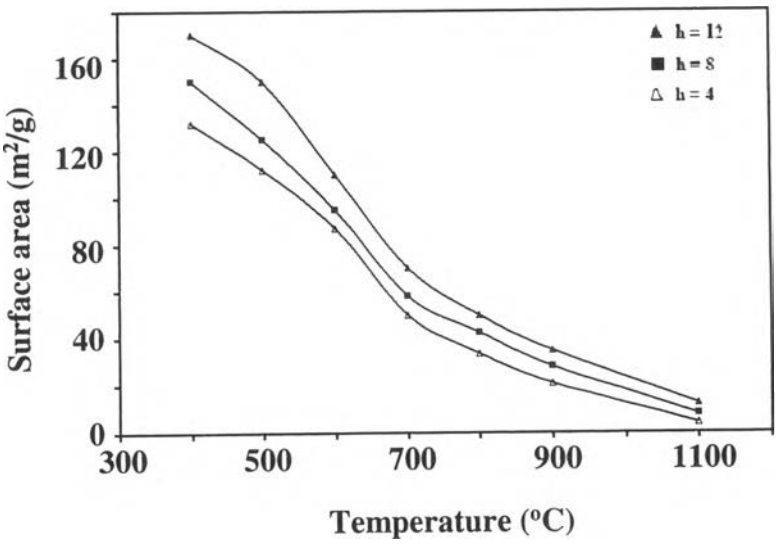

Figure 7. (Ksapabutr et al.)

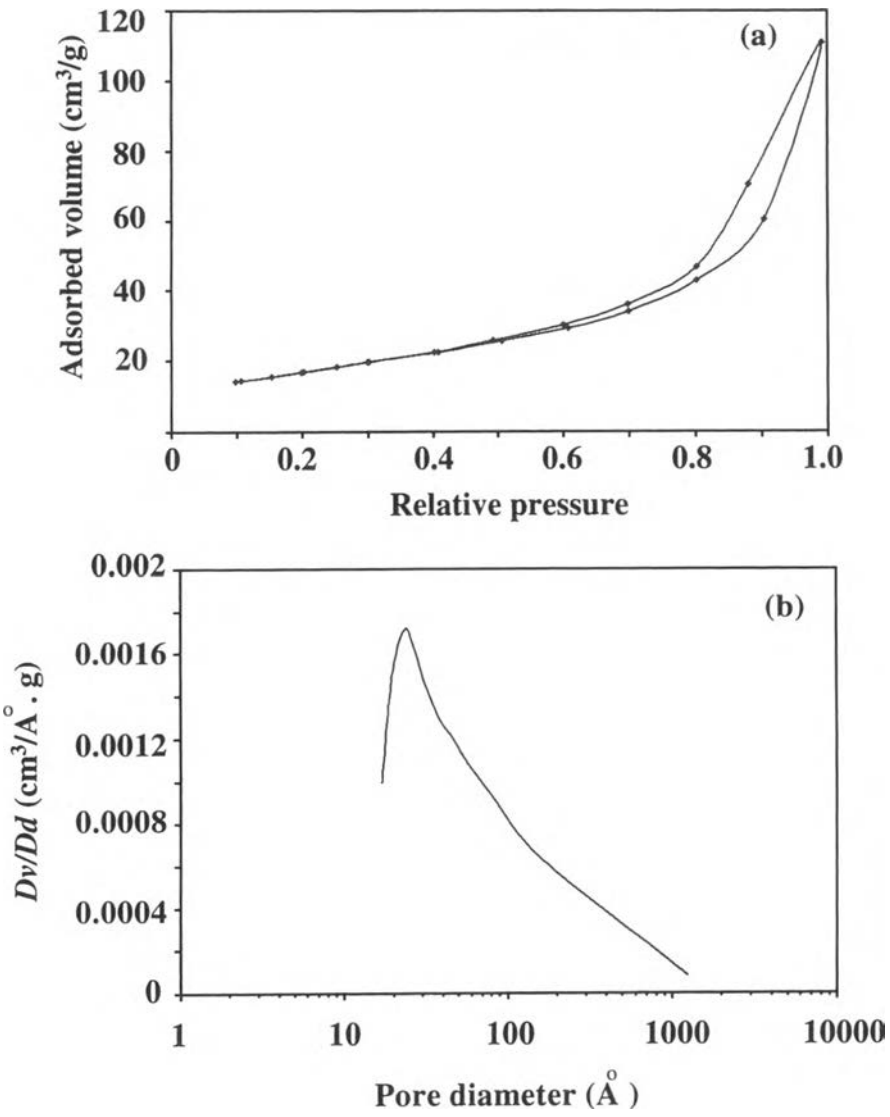

Figure 8. (Ksapabutr et al.)

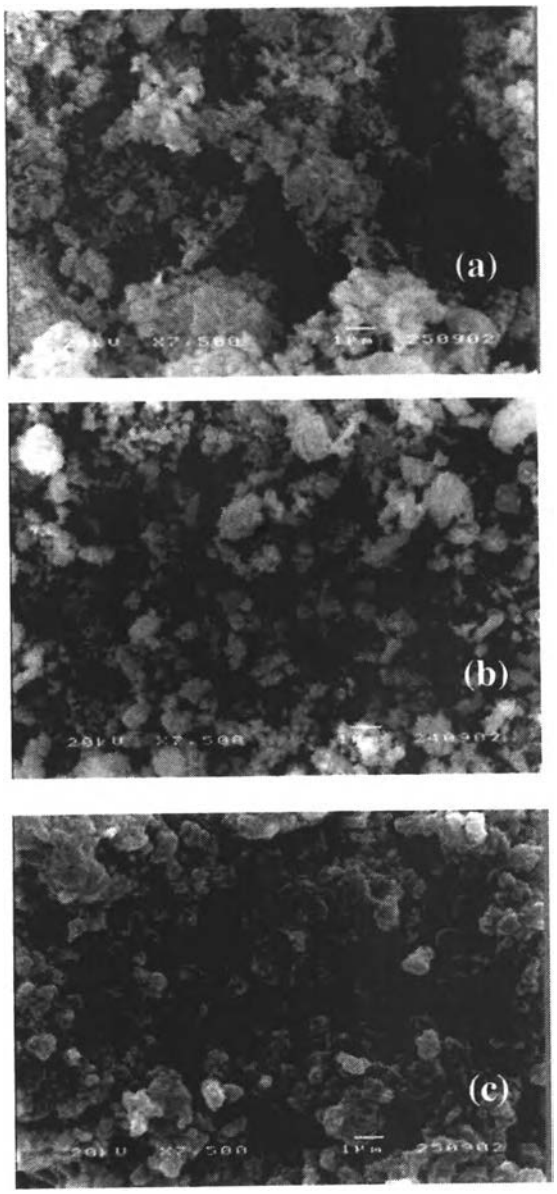

Figure 9. (Ksapabutr et al.)

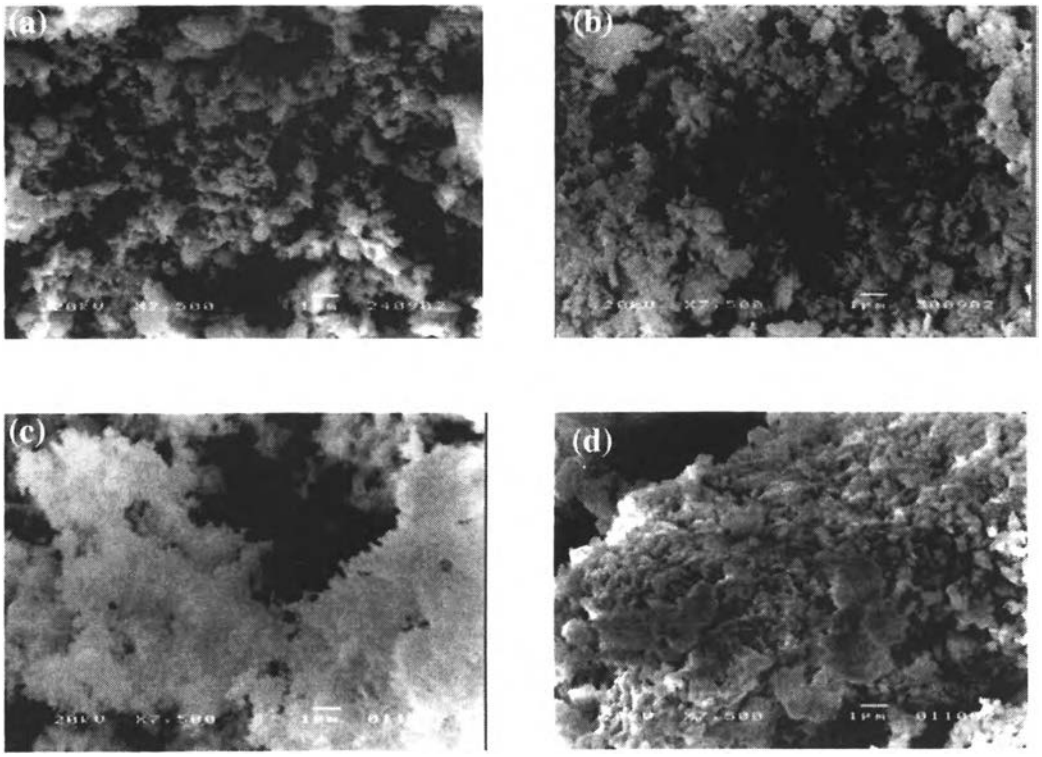

Figure 10. (Ksapabutr et al.)